Acta Biomaterialia 6 (2010) 4430–4438

Contents lists available at ScienceDirect

Acta Biomaterialia

journal homepage: www.elsevier.com/locate/actabiomat

Magnetic isolation of particles suspended in synovial fluid for diagnostics of natural joint chondropathies

Kalia Mendel [a], Noam Eliaz [a,*], Itai Benhar [b], David Hendel [c], Nahum Halperin [d]

[a] The Materials Science and Engineering Program, The Iby and Aladar Fleischman Faculty of Engineering, Tel-Aviv University, Ramat Aviv, Tel-Aviv 69978, Israel
[b] Department of Molecular Microbiology and Biotechnology, The George S. Wise Faculty of Life Sciences, Tel-Aviv University, Ramat Aviv, Tel-Aviv 69978, Israel
[c] Department of Orthopedics, The Edith Wolfson Medical Center, Holon 58100, Israel
[d] Department of Orthopedics, Assaf Harofeh Medical Center, Zerifin 70300, Israel

ARTICLE INFO

Article history:
Received 28 March 2010
Received in revised form 31 May 2010
Accepted 1 June 2010
Available online 8 June 2010

Keywords:
Bio-ferrography
Osteoarthritis
Immunochemistry
Magnetic labeling
Wear debris

ABSTRACT

Millions of people are stricken with the degenerative joint disease known as osteoarthritis. Osteoarthritis is associated with biochemical and mechanical processes, and is characterized by loss of articular cartilage and hypertrophy of bone. As cartilage and bone particles are released into the synovial fluid, a variety of biomarkers have been suggested for the analysis of this fluid. Here we have developed a method for isolating bone and cartilage wear particles suspended in the synovial fluid of the hip, knee and ankle joints of humans, based on specific magnetization of collagens I and II. Bio-ferrography is used to capture the particles on glass slides, allowing microscopic, chemical and statistical analyses. The relations between the level of the disease and the number, dimensions, shape and chemical composition of the particles were established. The method, which was found to be sensitive and reliable, can easily be extended to other applications, such as diagnosis of cancer and infectious diseases, determination of the efficacy of drugs or optimization of implants.

1. Introduction

Millions of people [1,2] are stricken with the degenerative joint disease known as osteoarthritis (OA). The main risk factors for OA are age, obesity, joint trauma and, sometimes, genetic abnormalities. OA is associated with biochemical and mechanical processes and is characterized by loss of articular cartilage and hypertrophy of bone. It is most common in certain joints, namely the knee, hip, hand and foot, and is the most common reason for total joint replacement. The clinical symptoms of OA are pain and functional impairment, including joint stiffness, a restricted range of motion, tenderness to palpation, crepitus during movement and swelling. If severe, the pathological changes result in morphological changes, such as narrowing of the joint space, subchondral bone sclerosis, formation of osteophytes and metaphyseal cysts [3]. Unfortunately, the symptoms often do not correlate well with the level of OA as determined radiographically [4,5]. More precise and sensitive measurements, such as magnetic resonance imaging (MRI) and computed tomography (CT), are still very expensive and not widely accessible. Therefore, alternative methods are needed that can detect osteoarthritic changes in the joints at an early stage of the disease in a reliable, sensitive, objective, quantitative and cost-effective manner.

The extracellular matrix of normal articular cartilage is composed mainly of water, collagens and proteoglycans. Collagen II represents approximately 90% of the overall content of collagen in the articular cartilage of adults, while being present at minor concentrations in other tissues [6]. The entire joint is surrounded by the synovium membrane, which produces the synovial fluid – a lubricating liquid that supplies nutrients and oxygen to cartilage. Both the synovial fluid and cartilage contain hyaluronic acid (HA), which has been claimed to provide lubrication, inhibit the synthesis of prostaglandin E2 (PGE2) and affect cell–cell interactions. HA levels are reduced in OA joints, thus intra-articular injections of exogenous HA are provided as compensation [7]. As cartilage and bone particles are released into the synovial fluid, a variety of biomarkers have been suggested for analysis of this fluid (as well as of serum and urine) [3,4,8].

Ferrography is a method of particles separation onto a glass slide based upon the interaction between an external magnetic field and the magnetic moments of the particles suspended in a flow stream. By determining the number, shape, size, texture and composition of particles on the ferrogram, the origin, mechanism and level of wear can be determined. The method was developed by Westcott et al. in the early 1970s to investigate the occurrence of ferrous wear particles in lubricated dynamic components [9–11], and has recently been reviewed [12,13]. Its success in engineering systems, allowing early wear detection and preventative maintenance, has led to its adaptation to other areas. Several feasi-

* Corresponding author. Tel.: +972 3 6407384; fax: +972 3 6407617.
E-mail address: neliaz@eng.tau.ac.il (N. Eliaz).

1742-7061/$ - see front matter © 2010 Acta Materialia Inc. Published by Elsevier Ltd. All rights reserved.
doi:10.1016/j.actbio.2010.06.003

bility studies have demonstrated its applicability to the study of arthritic human and sheep joints [14–20]. Ferrography was found to be very sensitive in monitoring articular erosion, with a resolution much greater than that of arthroscopy [15]. The main weaknesses of these studies were: (1) the use of a non-specific magnetization method (adsorption of the paramagnetic lanthanide cation Er^{3+}) [21,22], with troublesome precipitation and background deposits [15,18]; (2) the use of a conventional analytical ferrograph with near horizontal flow, which reduced the contribution of the magnetic force compared with the gravitational and hydrodynamic forces.

Bio-ferrography (BF) is a recent modification of conventional analytical ferrography that was specifically developed to allow magnetic isolation of target cells or tissues [23–26]. It exhibits a unique combination of strengths compared with other techniques commonly used in biotechnology (such as flow cytometers and sorters, high gradient magnetic cell concentration methods, monolayer cell preparation systems and automated slide stainers), including: (1) the ability to quantify biological matter and, at the same time, analyze its microscopic features; (2) preservation of the structure and morphology of the captured particles, which might otherwise not be observed if an acid dissociation step is required; (3) extremely high selectivity and sensitivity due to a vertical flow; (4) a requirement for less sample manipulation relative to conventional immunomagnetic separation techniques; (5) applicability to any liquid sample, including whole blood; (6) samples as small as 1 μl and target particles as small as several nanometers can be analyzed [27]; (7) the possibility to simultaneously process up to five samples within bracketed areas on a single slide, without cross-contamination.

So far, BF has been used to track *Escherichia coli* bacteria at low concentrations in natural waters [28–30], characterize biofilms within ships' water ballast tanks [31], separate breast cancer and other cells from human peripheral blood [32,33], separate polyethylene wear debris from hip simulator fluid [34], capture of carbon nanoparticles produced by a pulsed arc submerged in ethanol [27] and determination of the role of magnetic minerals embedded in the comb cells of Vespinae [35].

Here we have developed a method for isolating bone and cartilage wear particles suspended in the synovial fluid of human hip, knee and ankle joints by specifically labeling collagens I and II with monoclonal antibodies coupled to magnetic beads.

2. Materials and methods

2.1. Extraction of synovial fluids

The tests and protocols were approved by the Helsinki Committee of Assaf Harofeh Medical Center in October 2004. Synovial fluid aspirates were drawn from 14 patients in two hospitals, either during arthroscopy or during total joint replacement. The aspirates were stored in a freezer at −19 °C. The pathologies of the patients can be divided into 10 primary knee OA, 1 secondary knee OA, 2 primary hip OA and 1 secondary ankle OA. The patients were treated with non-steroidal anti-inflammatory drugs (NSAIDs), mainly aspirin, to relieve pain and reduce inflammation. Nutritional supplements, namely glucosamine sulfate or chondroitin sulfate, were also given. Physiotherapy was used to strengthen the muscles around the joint, increase the range of motion and reduce pain. Acupuncture was also used for short-term relief of pain.

2.2. Centrifugation of synovial fluids

The synovial fluids were defrosted and then centrifuged to separate the wear particles from the hyaluronic acid. Saline solution (0.9% NaCl) was added to each sample test tube using sterile disposable pipettes, equalizing the fluid volume in all tubes. Each test tube was vortexed for several seconds in order to attain a uniform solution, using a Stir Mixer 18000 instrument from Tuttnauer Co. Ltd. When necessary, shaking by hand was used to disintegrate solid aggregates. The test tubes were then centrifuged at 3200 r.p.m. and 4 °C for 15 min in a Sorvall RT6000B centrifuge. Most of the fluid above the sediment was withdrawn and saline solution was added. The centrifugation process was repeated twice more, each for 10 min. Finally, most of the fluid was withdrawn, 1 ml of saline was added to each test tube and vortexing was carried out in order to obtain uniform samples.

Although centrifugation was found to result in the loss of some wear particles, it was necessary to either make the synovial fluid less viscous, thus enabling flow through the ferrograph tubing, or prevent coagulation when $ErCl_3$ was used as the magnetizing agent. Future work may include seeking ways to eliminate the need for centrifugation, e.g. dilution of the synovial fluid with distilled water.

2.3. Magnetic labeling of wear particles

Wear particles were magnetically labeled with commercial monoclonal anti-collagen I and anti-collagen II antibodies coupled to nanometric paramagnetic beads. One of the control groups was magnetized with $ErCl_3$ solution.

Sample manipulation was done using powder-free latex disposable gloves in order to minimize sample contamination. Each of the centrifuged synovial fluid samples was divided into three Eppendorf burettes: (1) 0.2 ml sample + 0.8 ml distilled water + 2 μl anti-collagen I mouse antibody + 10 μl goat-anti-mouse magnetic beads; (2) 0.2 ml sample + 0.8 ml distilled water + 2 μl anti-collagen II mouse antibody + 10 μl goat-anti-mouse magnetic beads; (3) 0.2 ml sample + 0.8 ml $ErCl_3$ solution (10 mM). The distilled water was produced using a Milli-DI™ system from Millipore. The antibody solutions were centrifuged before addition to the burettes in order to reduce the amount of unused antibody. The anti-collagen I antibody was purchased from Sigma (COL-1, product No. C-2456), whereas the anti-collagen II antibody was purchased from ICN (Clone II-4CII, product No. 63171). A Biohit Proline micro-pipetor was used to transfer exact volumes. The goat-anti-mouse IgG MACS MicroBeads solution was purchased from Miltenyi Biotec (product No. 130-048-401). The beads were 50 nm in diameter. The $ErCl_3$ powder was purchased from Sigma–Aldrich (product No. 32,559–7, erbium(III) chloride, anhydrous, 99%) and dissolved in distilled water.

2.4. Bio-ferrography (BF)

The Bio-Ferrograph 2100 system from Guilfoyle, Inc. [23–26], which was used in this work, is a benchtop cytometry-based instrument (Fig. 1a). It utilizes a magnetic field that has maximum field strength across an interpolar gap, where the collection of magnetically susceptible particles takes place. The maximum magnetic field strength across the gap is 1.8 T. However, the gradient of that field is maximal at the edges of the gap, where deposition is concentrated (Fig. 1b). In order to minimize contamination of the samples by the surroundings, the bio-ferrograph was placed in a biological safety cabinet (ADS Laminar's Optimale 12).

The capture (i.e. towards the syringes) flow rate was fixed at 28 μl min^{-1}, which was found to be sufficiently slow to ensure effective adsorption of antibodies. In all cases, a washing step was included to remove residues of sample fluid from the cassette. At an early stage of the work saline solution was used for washing. However, this resulted in precipitation of salt crystals on the ferrogram, which masked some of the wear particles during scanning

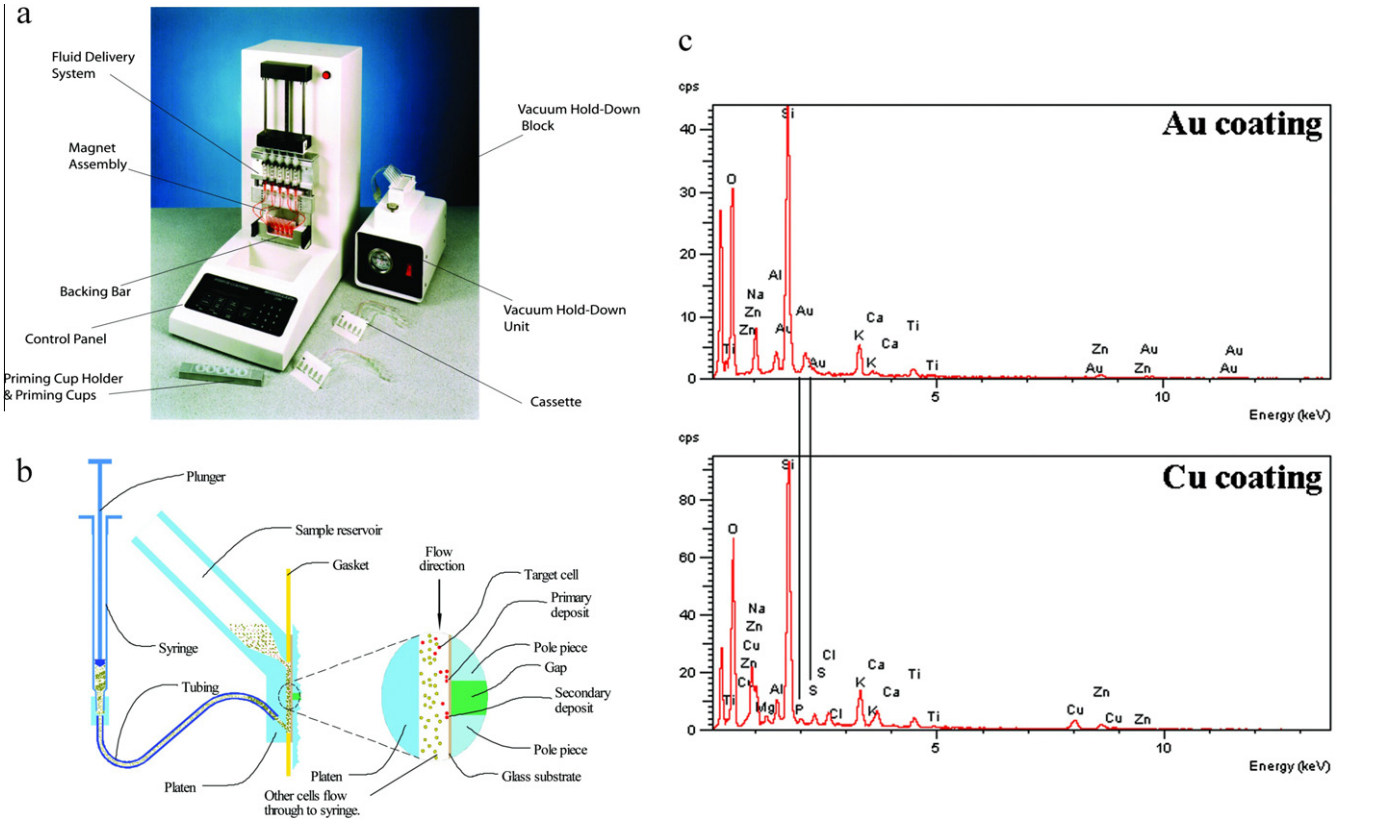

Fig. 1. The principles of bio-ferrography: (a) Bio-Ferrograph 2100 (Guilfoyle, Inc.), the platform used to deposit magnetically tagged particles of cartilage and bone onto a glass slide [24,26]; (b) the deposition scheme of captured particles on the slide [26]; (c) EDS spectrum from wear particles on ferrograms coated with either gold or copper.

electron microscopy (SEM) imaging and interfered with the chemical analysis. Hence, a change to washing with distilled water was made. The fragile glass substrate (ferrogram) was removed from the remaining parts of the cassette by means of a dedicated vacuum hold-down unit (Fig. 1a). Finally, it was allowed to naturally dry for several minutes inside the safety cabinet.

2.5. Staining

At an early stage of the work several staining protocols were evaluated. These included a fluorescent antibody (fluorescein (DTAF)-conjugated AffiniPure rabbit anti-mouse IgG (H + L) from Immuno Research Laboratories) as well as different dyes (Alcian Blue for cartilage, Alizarin Red and Von Kossa for bone). The fluorescent antibody was found not to be useful because part of it conjugated the magnetic beads, thus introducing fluorescence around beads that were not linked to wear particles. It was also found that $ErCl_3$ magnetized the fluorescent antibody, thus introducing overall fluorescence and masking the glare of wear particles. The $ErCl_3$ solution also reacted with Alizarin Red and Alcian Blue, introducing background staining. In the presence of magnetic beads the surrounding tissue, and sometimes the glass slide, was stained, thus masking the wear particles. A possible explanation for these interactions is suggested. Alcian Blue has a positive charge and competes for the same anionic sites, mainly proteoglycans in the cartilage matrix, as the erbium cation. Therefore, a sufficiently high quantity of either Alcian Blue or $ErCl_3$ will block the other. Alizarin Red has a negative charge and stains bone by bonding to the calcium cation in hydroxyapatite (HAp). However, due to its opposite charge it may bond to Alcian Blue, if they are mixed together. The erbium cation may behave as an "improved" calcium cation, hence its presence may significantly increase staining by Alizarin Red. If sufficient erbium magnetizes cartilage, staining by Alizarin Red may occur, giving the wrong impression of a bone particle. The Von Kossa stain was found to be non-specific; it seemed not to mark wear particles in a clear manner.

2.6. Validation of bio-ferrographic observations – controls

The size and morphology of wear particles captured in this study were compared with those typical of dust, aerosols and pollution particles. Images of typical pollution particles were reported by Bowen and Westcott [36]. In addition, a ferrogram prepared by running distilled water without synovial fluid revealed neither a capture band nor any particles similar to those captured from synovial fluid. Based on these comparisons, it was concluded that the source of the captured particles in this study was the synovial fluid (and not the room environment, water system, etc.).

2.7. Scanning electron microscopy (SEM)

Most of the characterization was done in a JEOL JSM-6300 microscope. Complementary characterization was carried out in a JEOL JSM-5600 microscope, as well as in a FEI Quanta 200 environmental scanning electron microscope. The attached energy dispersive X-ray spectroscopy (EDS) was used for chemical analysis. Most particles smaller than 5 μm were not characterized due to limitations of the sampling volume ("onion") in EDS analysis. Bone is composed of inorganic (mineral) and organic constituents, the former representing around 69 wt.% of wet cortical bone. The primary inorganic constituent of all mammalian skeletal tissues is apatite, mainly HAp ($Ca_5(PO_4)_3(OH)$) [37,38]. Hence, calcium (Ca) and phosphorous (P) may be used in chemical analysis to identify bone particles (Ca/P = 1.67 in stoichiometric HAp and around 1.60 in

biological HAp) [16]. Articular cartilage is a type of hyaline cartilage. This tissue consists of chondrocytes embedded in an extracellular matrix (ECM), whose two primary load-bearing macromolecules are collagen II and the chondroitin sulfate proteoglycan 'aggrecan' [37]. Due to its aggrecan content, cartilage normally contains appreciable amounts of sulfur (S), although these decline markedly in arthritic lesions [16,39]. The zone of calcified cartilage forms an important interface between cartilage and bone in transmitting force, attaching cartilage to bone and limiting diffusion from bone to the deeper layers of cartilage [39]. It contains Ca and P in addition to S [16]. To summarize, a high S content is expected in cartilage particles, a high Ca content is expected in bone particles and a high content of both elements is expected in calcified cartilage. SEM imaging first required coating the ferrogram with a conductive coating. During the work it was found that the M_α peak of gold (Au) masked the K_α peak of S (as well as other relevant peaks, such as P). The gold coating also resulted in suppression of Ca and Mg peaks compared with the background. Similar effects have been reported for characterization of dust particles [40], but were nevertheless overlooked in all previous reports on ferrography as well as in many papers dealing with bone and cartilage particles in general. Copper (Cu) coating was found to be a successful alternative, revealing S and P peaks that were otherwise masked (Fig. 1c). Copper sputtering was done for 13–18 s at 100 W under an argon atmosphere at a pressure of $\sim 10^{-2}$ torr. The resulting coating was 150–200 Å thick. The first stage was to construct an atlas of biological wear particles, equivalent to that used for engineering systems in aircraft [36]. All particles were sorted into one of the five following shapes: chunky, platelet, rod-like, fibers or irregular shapes.

2.8. Numeric description of wear particles and statistical tests

The area (A), perimeter (P) and length (L) [18,41] of each particle were measured on SEM binary images by means of analySIS Docu v. 3.2 software from Soft Imaging System GmbH. The width (W), shape factor (SF), elongation (Δ) and roundness (R) were subsequently calculated from the relations [41]:

$$W = \frac{4A}{\pi L} \tag{1}$$

$$SF = \frac{4\pi A}{P^2} \tag{2}$$

$$\Delta = \frac{L}{W} \tag{3}$$

$$R = \frac{4A}{\pi L^2} \tag{4}$$

ANOVA parametric statistical tests were performed with the aid of SPSS v. 11 software.

2.9. Light microscopy

An Olympus model IX71 inverted microscope with bichromatic illumination, adapted for both biological and metallurgical samples, was used. Imaging was done under bright field illumination, polarized light and differential interference/Nomarski contrast (DIC). Because some of the biological matter is transparent to visible light, bright field illumination is insufficient. Imaging under polarized light adds information on the optical activity of different particles, and has become widespread in the study of cartilage (all fibrous structures are birefringent objects; cartilage is a very non-homogeneous and anisotropic tissue). The Nomarski image allows differentiation between particles with different chemical compositions thanks to the different colors observed. Most images were acquired at 200× magnification. Samples that did not require further SEM/EDS analysis were preserved by drying the ferrogram with xylene, dripping on several drops of Entellan New from Merck (product No. 107961) and bonding to a Menzel-Glaser SuperFrost Plus slide, which served as a coverglass.

2.10. Induction coupled plasma atomic emission spectroscopy (ICP-AES)

Four samples of synovial fluid from three different patients were analyzed with a Spectroflame EOP FSPEA83C system from Spectro Analytical Instruments in order to determine the composition of the synovial fluid before and after centrifugation. Sample preparation consisted of either oxidation (in a solution of nitric acid with hydrogen peroxide) or more aggressive microwave irradiation (at 170–180 °C and 200 atm). The concentrations of different elements in the fluid were determined through calibration with certified single element reference standards containing different concentrations of the elements of interest. The ICP-AES tests showed that Na, K, Ca, S, Zn, P, Mg, Fe, Cu and Al were present in the as-drawn synovial fluid and that centrifugation resulted in a decrease of more than one order of magnitude in the concentrations of Ca, P and S. For example, when preparing the sample by etching, the Ca, P and S concentrations were decreased from 24.2, 21.9 and 167.2 ppm to 1.6, 0.8 and 9.5 ppm, respectively, as a result of centrifugation. An example of the Ca and S signals from one of the synovial fluid samples after centrifugation and microwave irradiation is shown in Fig. 2, in comparison with the signals from different calibration solutions.

2.11. Radiological assessment

The radiological assessment was conducted in hospitals, independently of the work in the laboratory, and its results were provided by orthopedic specialists at the end of the research, to avoid any possible bias in ferrographic evaluation.

3. Results and discussion

Bio-ferrography was used to capture the particles on glass slides, allowing microscopic, chemical and statistical analysis. Fig. 3 shows typical SEM images of bone particles captured due to their collagen I content, cartilage particles captured due to their collagen II content and cartilaginous particles captured due to their collagen I content. Light microscopy images of some of the particles are also shown. Bone particles were mostly angular, with either a crystalline or spongy appearance; the latter may be attributed to the trabecular structure of bone. Most of them were characterized under polarized light by high optical activity, which may be related to their crystalline structure. The shape of cartilage wear particles may be related to their origin within the tissue [42]. For example, it is expected that wear of the surface layer of cartilage (lamina splendens), which consists of collagen leaves with no bridging fibrils, will generate platelet particles in patients with a lower grade of OA [18]. Such particles exhibited low optical activity (bluish-silvery color). In contrast, chunky particles will be generated in patients with a higher grade of OA from the deeper zones of cartilage, where a network of bridging fibrils exists. During advanced stages of the disease irregular shapes are also common [18].

The origin of each particle was determined based on its chemical composition and the channel on the ferrogram on which it was captured as follows.

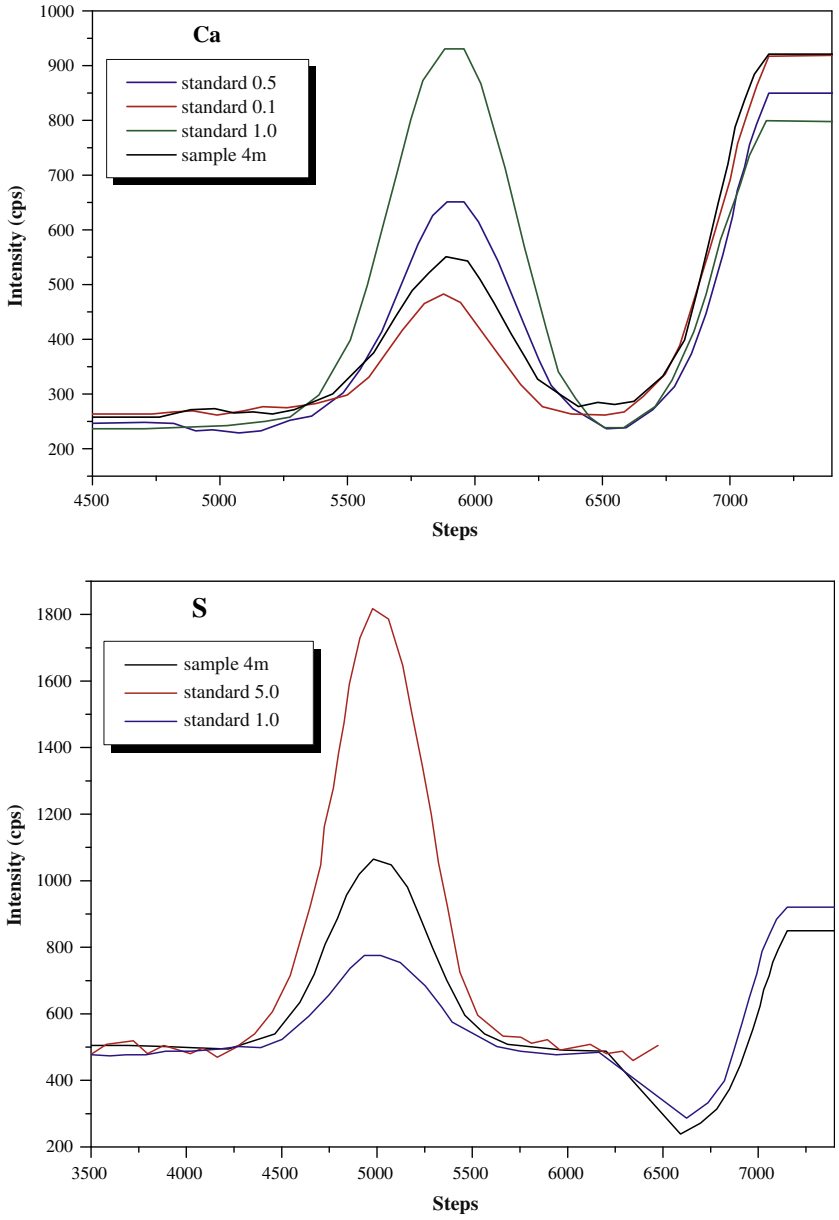

Fig. 2. ICP-AES signals of Ca and S in synovial fluid after centrifugation and microwave irradiation, in comparison with the signals from different calibration solutions.

1. Particles rich in Ca and in collagen I: subchondral bone fragments.
2. Particles rich in Ca and in collagen II: the interface between subchondral bone and calcified cartilage.
3. Particles rich in S and in collagen II: articular cartilage fragments.
4. Particles rich in S and in collagen I: repaired cartilage, calcified cartilage, degenerate cartilage, synovium or meniscus fragments (the latter is relevant to knee joints only). These particles were referred to as "cartilaginous particles".
5. Particles containing neither Ca nor S (typically consisting of only Mg, P or C): uncertain origin.

The Mg-rich particles could have formed during either biochemical dissolution of bone or selective precipitation from body fluids. ICP-AES measurements proved that Mg was present in the synovial fluids of these patients, as drawn. It has been reported that magnesium whitlockite may play a pathological role in arthritis [43,44]. Magnesium has been detected in the synovial fluids of patients suffering from either OA or rheumatoid arthritis [45]. Thus, further in-depth characterization of these particles may shed more light on the biochemical processes involved in arthritis. Regarding particles rich in Ca and in collagen II, Oegema et al. suggested that the biomineralization process is accompanied by a significant drop in the content of proteoglycans [39], which is expected to result in a decrease in the concentration of S compared with Ca. The minimal Ca/S mass ratio of an unambiguously identified bone particle was 4.08 (when taking into account also P and Mg). As Mg and P were present in most particles captured based on either collagen I or collagen II, they could not be referred to as indicative of the bone mineral. A mass ratio Ca/S < 1.0 was found to be representative of cartilage particles. Finally, in some cases amorphous deposits with no optical activity were observed on the ferrograms, mainly within flow channels with anti-collagen I antibody. These deposits were identified as fragments of the synovial tissue, which is known to contain both collagen I and collagen III [16].

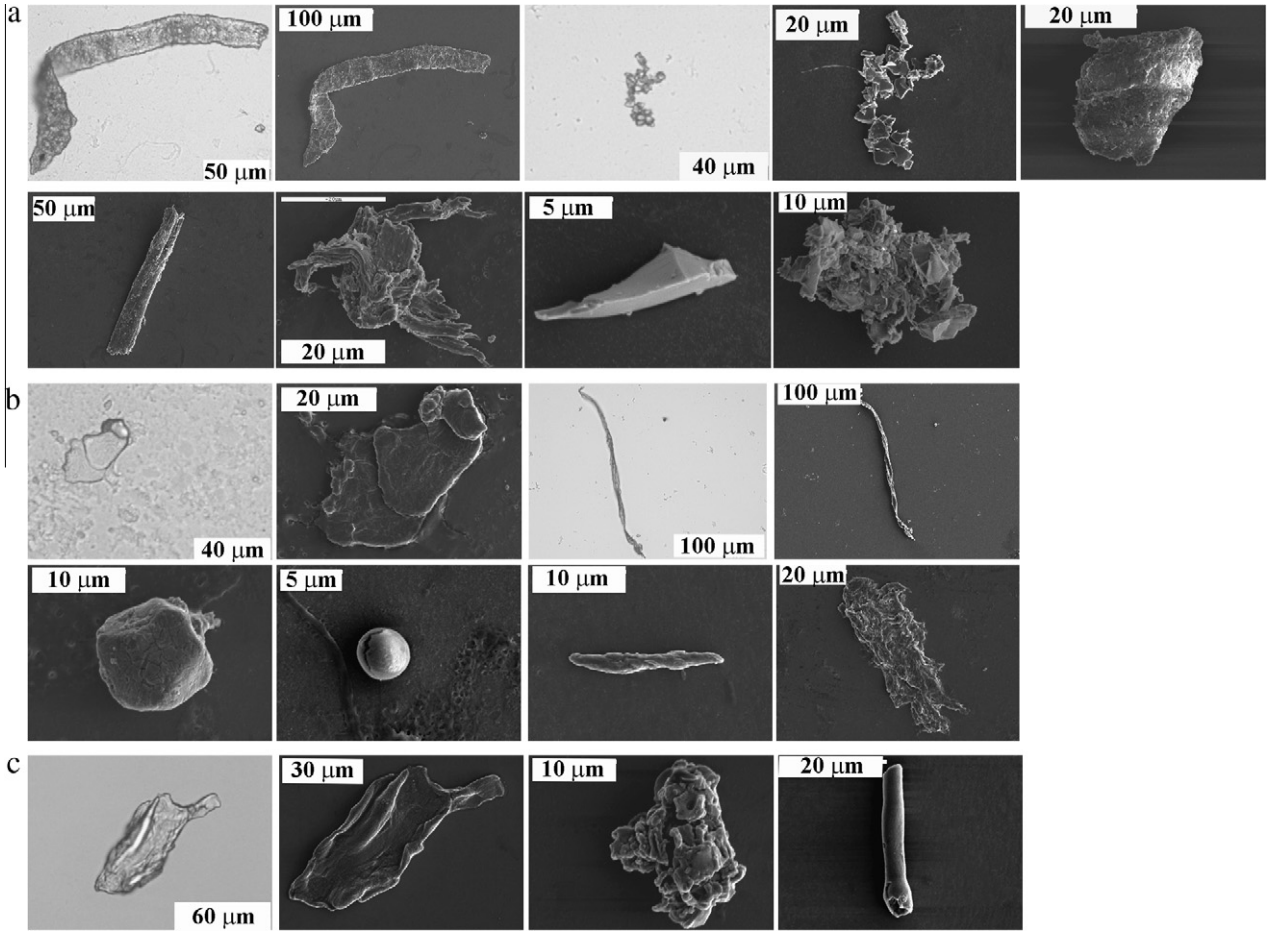

Fig. 3. Typical wear particles isolated from the synovial fluid of humans, as observed by SEM and light microscopy. (a) Bone particles rich in collagen I (9 images); (b) cartilage particles rich in collagen II (8 images); (c) cartilaginous particles rich in collagen I (4 images). Numbering from top left to bottom right: images a1, a3, b1, b3 and c1 are light microscope images. All other images are SEM images.

The Kellgren and Lawrence scheme was used to grade the severity of OA based on radiographs, from 0 (normal) to 4 (most severe) [46]. The average area, maximal area, average length and maximal length of cartilage particles (category 3) were found to increase as the level of OA increased (Table 1). Ferrograms of patients that were graded as Kellgren 4 contained a significantly higher number of cartilage wear particles. For each grade of OA there were always fewer bone particles than cartilage particles (Table 1). The number of bone particles was significantly higher in the case of Kellgren 4 than in lower grades of OA. In the case of Kellgren 1 no bone particles were detected. The average length and average shape factor of bone particles increased with the severity of disease. Thus, the assessment of natural joint degradation by BF was usually supported by the clinical diagnosis. Nevertheless, in several cases the high sensitivity of BF enabled detection of wear particles in the synovial fluid which were not expected based on arthroscopic evaluation. This may be explained by the higher magnification at which the particles were observed on the ferrogram and by the higher sensitivity of monitoring separate wear debris compared with inspection of a bulk material.

The number of wear particles captured in this research by means of BF and specific labeling of target collagens was much

Table 1
Correlations between the grade of osteoarthritis and the number, dimensions and shapes of cartilage particles captured based on collagen II and bone particles captured based on collagen I.

Kellgren grade	No. of particles	Area (μm^2)		Length (μm)		Shape factor	
		Average	Range	Average	Range	Average	Range
Cartilage							
1	24	307.3	38.4–923.0	27.9	9.7–52.3	0.44	0.08–0.75
2	92	491.8	1.4–4800.7	32.9	1.4–132.8	0.48	0.11–0.83
3	29	512.6	2.1–6779.8	35.0	1.8–185.6	0.49	0.07–0.90
4	156	648.8	7.4–8768.0	37.1	4.3–234.0	0.48	0.11–0.87
Bone							
1	0						
2	17	155.2	9.2–750.6	18.5	4.9–67.5	0.44	0.24–0.85
3	3	478.1	32.8–977.3	30.8	9.4–45.1	0.45	0.35–0.57
4	62	437.0	5.7–6534.2	33.5	3.1–309.8	0.51	0.09–0.83

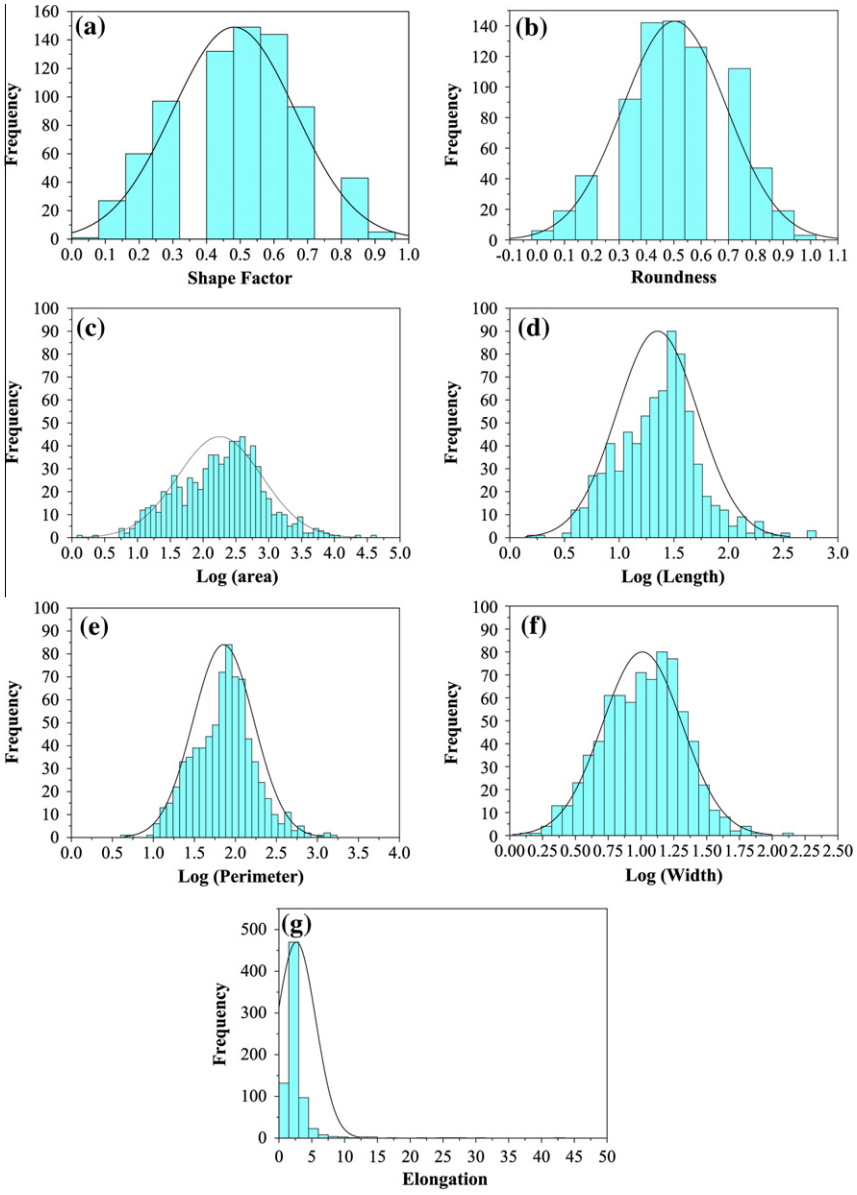

Fig. 4. Quantitative image analysis and statistical analysis of wear particles captured by bio-ferrography ($n = 751$). (a) Distribution of the particle shape factor (mean ± SD = 0.481 ± 0.182, min = 0.0, max = 0.9); (b) distribution of the particle roundness (mean ± SD = 0.503 ± 0.190, min = 0.0, max = 1.0); (c) distribution of the particle area after logarithmic transformation (mean ± SD = 2.255 ± 0.643, min = 0.13, max = 4.59); (d) distribution of the particle length after logarithmic transformation (mean ± SD = 1.350 ± 0.371, min = 0.16, max = 2.79); (e) distribution of the particle perimeter after logarithmic transformation (mean ± SD = 1.855 ± 0.371, min = 0.66, max = 3.19); (f) distribution of the particle width after logarithmic transformation (mean ± SD = 1.009 ± 0.304, min = 0.08, max = 2.14); (g) distribution of the particle elongation (mean ± SD = 2.642 ± 2.947, min = 1.0, max = 42.8).

higher compared with the numbers in previous studies in which conventional analytical ferrography and non-specific labeling by $ErCl_3$ were used [15,18]. In those studies the statistical analysis was consequently limited.

The size of wear particles captured in this research, on the other hand, was smaller than in previous studies. A possible reason for this difference is the absence of a masking effect of salt crystals (e.g. NaCl from saline or $ErCl_3$), as well as of Au deposition on the ferrogram before SEM imaging in the present study. In addition, the effect of instrumentation and the associated deposition scheme should be taken into account. In conventional analytical ferrography three types of forces act on the suspended particles: magnetic, hydrodynamic (drag) and gravitational. Depending on the size of the particles, they may behave either as saturated magnetically (small particles) or as soft magnets (large particles). In addition to the magnetic force tending to accelerate the particles, drag forces retard their motion. The magnet of the ferrograph was designed to develop an extremely high gradient of magnetic field near the magnet poles. The ferrogram was mounted at a slight angle to the horizontal, with the entry end elevated so that the fluid flowed downward. Because the distance from the magnet to the substrate was slightly greater at the entry side than at the exit side, the magnetic field strength was weaker at the entry side, causing only the largest (magnetically affected) particles to deposit. Farther down the ferrogram the progressively stronger magnetic field deposited progressively smaller particles [9,13]. In contrast, in bio-ferrography a stronger magnet is used, the flow is vertical and the ferrogram is very thin (thus, the deposition surface is close to the interpolar gap). A very high magnetic flux density was established at the interpolar gap, generally around 1.8 T. The vertical

flow separated the vertical gravitational force from the nearly horizontal magnetic force, so that only the latter acted to retain magnetic particles moving downward through the flow chamber [23,25]. This deposition scheme resulted in elimination of gradual deposition of particles according to their size, while providing higher sensitivity and an ability to capture smaller particles (with lower magnetic moment).

For further statistical analysis the shapes of the distributions of the particles' area, length, perimeter, width, elongation, roundness and shape factor were determined (for $n = 751$ wear particles). While the shape factor (Fig. 4a) and roundness (Fig. 4b) exhibited normal distributions, the area, length, perimeter and width plots required logarithmic transformation in order to obtain normal distributions (Fig. 4c–f). The elongation (Fig. 4g), on the other hand, did not behave normally either before or after transformation.

One-way ANOVA tests of different particle shapes, followed by Scheffé post-hoc test, revealed differences in the measured shape parameters. The maximal area of chunky particles was 2.5 times larger in patients graded as Kellgren 4 than in other patients. The average area and maximal area of platelet particles were approximately twice as large and the minimal area 3.3 times larger in patients graded as Kellgren 4. The maximal area of rod-like particles was 2.7 times larger and the minimal area 4.4 times smaller in patients graded as Kellgren 4. These results represent a wider range of shape parameter values in patients graded as Kellgren 4 compared with other patients. The maximal area of fiber particles was 1.5 times smaller and the minimal shape factor 1.7 times larger in patients graded as Kellgren 4. In the case of irregular shaped particles no significant differences in shape parameters were observed in patients with different levels of OA. Some of the significant differences that were observed in shape parameters are summarized in Table 2.

One-way ANOVA tests, followed by a Scheffé post-hoc test, allowed a distinction between the characteristic shape parameters of bone and cartilage/cartilaginous particles. The area, perimeter and width of cartilage/cartilaginous particles were significantly different from those of either particles of uncertain origin or bone particles ($P < 0.01$). The roundness of the cartilage/cartilaginous particles was significantly different from that of bone particles ($P < 0.01$).

Univariate ANOVA showed that, as the level of OA increased bone and chunky (as well as rod-like) cartilage particles became more prominent (Fig. 5). It is evident that bone particles are generated at a higher grade of disease compared with cartilage particles. This was expected because at higher grades of the disease there was less cartilage present overall, hence the contacting surfaces were much less cartilage on cartilage or even cartilage on bone and much more bone on bone. It is also evident that chunky cartilage particles are related to higher grades of OA compared with platelet cartilage particles, in accordance with the three-dimensional architecture of collagen [42]. The trends for particles of uncertain origin, which were more similar to those of bone particles than to those of cartilage, support the hypothesis that the source of Mg-rich particles was bone.

In summary, we have developed a protocol for isolating bone and cartilage wear particles suspended in the synovial fluid of the hip, knee and ankle joints of humans, based on specific magnetization of collagens I and II and using bio-ferrography. Future extension of this research may include the use of more specific biomarkers, such as matrix metalloproteinases, interleukins, prostaglandins, telopeptides, cartilage oligomeric matrix protein (COMP) and neo-epitopes [3,4,8]. The combination of multiple markers holds the promise of increasing disease or tissue specificity. Other possible extensions include the study of the morphological and chemical changes in repaired cartilage compared with articular cartilage, in-depth investigation of the particles of uncertain origin in an attempt to better understand the underlying processes in osteoarthritis, comparison between primary and secondary OA and controlled animal studies of homogeneous test groups and healthy joints. The latter will enable the elimination of any possible effects of medication and physical therapy. Although the procedure was demonstrated for osteoarthritis, it can easily be applied to the investigation and diagnosis of other joint diseases. There is also great interest in developing

Table 2
Statistical comparisons between the numeric shape parameters for different shapes of wear particles.

Numeric shape parameter	Shape 1	Shape 2	Significance (P)
Log area	Chunky	Rod-like	0.342
		Plate	0.000
		Fiber	0.000
		Irregular shape	0.000
	Rod-like	Chunky	0.342
		Plate	0.040
		Fiber	0.000
		Irregular shape	0.340
Log perimeter	Chunky	Rod-like	0.012
		Plate	0.000
		Fiber	0.000
		Irregular shape	0.000
Log length	Chunky	Rod-like	0.000
		Plate	0.000
		Fiber	0.000
		Irregular shape	0.000
Log width	Plate	Chunky	0.000
		Rod-like	0.000
		Fiber	0.416
		Irregular shape	0.184
Shape factor	Chunky	Rod-like	0.000
		Plate	0.001
		Fiber	0.000
		Irregular shape	0.000
	Plate	Chunky	0.001
		Rod-like	0.000
		Fiber	0.000
		Irregular shape	0.000
Roundness	Chunky	Rod-like	0.000
		Plate	0.000
		Fiber	0.000
		Irregular shape	0.000
	Plate	Chunky	0.000
		Rod-like	0.000
		Fiber	0.000
		Irregular shape	0.000

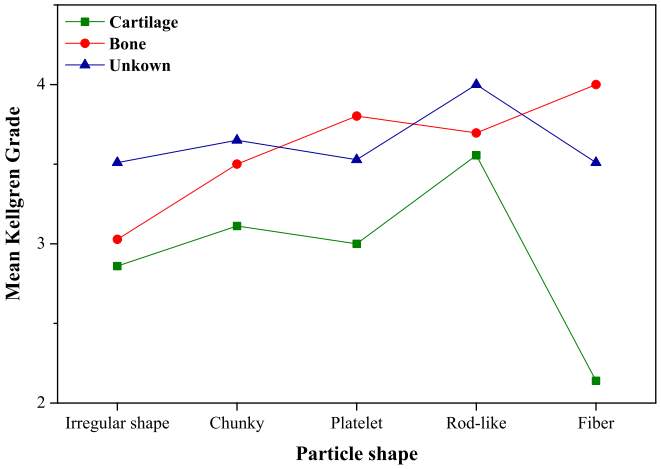

Fig. 5. Univariate ANOVA revealing the correlation between the chemical composition and shape of wear particles captured by bio-ferrography and the Kellgren grading of osteoarthritis.

new diagnostic techniques for cancer and infectious diseases. Such techniques should ultimately be helpful in studying the processes and underlying mechanisms of the diseases, and should involve minimum discomfort to the patient. Bio-ferrography satisfies these needs. It could also be very powerful in determining the efficiency of drugs and other clinical treatments in a sensitive, objective and timely manner. For example, we have recently completed a study of the efficacy of hyaluronan injections in treating osteoarthritic human knees. The technique could also be powerful in monitoring the wear of artificial joints, either in service or during the development stage, in which different materials and geometries are considered. Excessive wear often causes pain following arthroplasty. The latter two applications have also been studied in our laboratory. Finally, the principles of bio-ferrography may be integrated into a microfluidics platform combined with non-magnetic detection techniques in order to further improve the sensitivity and selectivity of the technique, allow for simultaneous analysis of more samples and make it portable.

4. Conclusions

A method for isolating bone and cartilage wear particles suspended in the synovial fluid of the hip, knee and ankle joints of humans, based on specific magnetization of collagens I and II, was developed. Bio-ferrography was used novelly to capture the particles on glass slides, thus allowing microscopic, chemical and statistical analysis. The relations between the level of the disease and the number, dimensions, shape and chemical composition of the particles were established. The method, which was found to be sensitive and reliable, can easily be extended to other applications, such as the diagnosis of cancer and infectious diseases, determination of the efficacy of drugs or optimization of implants.

Acknowledgements

The authors thank Gilad Golub of the Environmental Services Company Ltd for the ICP-AES measurements. The authors also thank Christopher Evans and John Desjardins for useful discussions and comments.

Appendix A. Figures with essential color discrimination

Certain figures in this article, particularly Figures 1, 2, 4, and 5, are difficult to interpret in black and white. The full color images can be found in the on-line version, at doi:10.1016/j.actbio.2010.06.003.

References

[1] Arthritis Program. Arthritis related statistics. Atlanta, GA: Centers for Disease Control and Prevention; 2008. Available from: http://www.cdc.gov/arthritis/data_statistics/arthritis_related_statistics.htm.
[2] Arthritis Research Campaign. UK arthritis facts – at a glance. Chesterfield, UK: Arthritis Research Campaign; 2008. Available from: http://www.arc.org.uk/arthinfo/documents/UK%20Arthritis%20Facts.pdf.
[3] Wieland HA, Michaelis M, Kirschbaum BJ, Rudolphi KA. Osteoarthritis – an untreatable disease. Nat Rev Drug Discov 2005;4:331–44.
[4] DeGroot J, Bank RA, Tchetverikov I, Verzijl N, TeKoppele JM. Molecular markers for osteoarthritis: the road ahead. Curr Opin Rheumatol 2002;14:585–9.
[5] Hannan MT, Felson DT, Pincus T. Analysis of the discordance between radiographic changes and knee pain in osteoarthritis of the knee. J Rheumatol 2000;27:1513–7.
[6] Eyre D. Review: Collagen of articular cartilage. Arthritis Res 2002;4:30–5.
[7] Brandt KD, Smith Jr GN, Simon LS. Intraarticular injection of hyaluronan as treatment of knee osteoarthritis: what is evidence? Arthritis Rheum 2000;43:1192–203.
[8] Herrero-Beaumont G et al. Cartilage and bone biological markers in the synovial fluid of osteoarthritic patients after hyaluronan injections in the knee. Clin Chim Acta 2001;308:107–15.
[9] Seifert WW, Westcott VC. A method for the study of wear particles in lubricating oil. Wear 1972;21:27–42.
[10] Scott D, Seifert WW, Westcott VC. The particles of wear. Sci Am 1974;230:88–97.
[11] Reda AA, Bowen R, Westcott VC. Characteristics of particles generated at the interface between sliding steel surfaces. Wear 1975;34:261–73.
[12] Eliaz N, Latanision RM. Preventative maintenance and failure analysis of aircraft components. Corros Rev 2007;25:107–44.
[13] Levi O, Eliaz N. Failure analysis and condition monitoring of an open-loop oil system using ferrography. Tribol Lett 2009;36:17–29.
[14] Mears DC, Hanley EN, Rutkowski R, Westcott VC. Ferrography: its application to the study of human joint wear. Wear 1978;50:115–25.
[15] Evans CH, Mears DC, Stanitski CL. Ferrographic analysis of wear in human joints: evaluation by comparison with arthroscopic examination of symptomatic knees. J Bone Joint Surg 1982;64:572–8.
[16] Evans CH. Application of ferrography to the study of wear and arthritis in human joints. Wear 1983;90:281–92.
[17] Podsiadlo P, Kuster M, Stachowiak GW. Numerical analysis of wear particles from non-arthritic and osteoarthritic human knee joints. Wear 1997;210:318–25.
[18] Kuster MS, Podsiadlo P, Stachowiak GW. Shape of wear particles found in human knee joints and their relationship to osteoarthritis. Br J Rheumatol 1998;37:978–84.
[19] Mills GH, Hunter JA. A preliminary use of ferrography in the study of arthritic diseases. Wear 1983;90:107–11.
[20] Graindorge SL, Stachowiak GW. Changes occurring in the surface morphology of articular cartilage during wear. Wear 2000;241:143–50.
[21] Evans CH, Tew WP. Isolation of biological materials by use of erbium (III)-induced magnetic susceptibilities. Science 1981;213:653–4.
[22] Evans CH, Russel AP, Westcott VC. Approaches to paramagnetic separations in biology and medicine. Part Sci Technol 1989;7:97–109.
[23] Seifert WW, Westcott VC, Desjardins JB. Flow unit for ferrographic analysis. US Patent No. 5714059; 1998.
[24] Guilfoyle, Inc.. New on the market: Bio-Ferrograph 2100. Nature 2000;407:818.
[25] Desjardins JB, Seifert WW, Wenstrup RS, Westcott VC. Ferrographic apparatus. US Patent No. 6303030; 2001.
[26] Guilfoyle, Inc.. Bio-Ferrograph 2100 users manual. Belmont, MA: Guilfoyle, Inc.; 2001.
[27] Parkansky N et al. Magnetic properties of carbon nano-particles produced by a pulsed arc submerged in ethanol. Carbon 2008;46:215–9.
[28] Zhang P, Johnson WP, Rowland R. Bacterial tracking using ferrographic separation. Environ Sci Technol 1999;33:2456–60.
[29] Zhang P, Johnson WP. Rapid selective ferrographic enumeration of bacteria. J Magn Magn Mater 1999;194:267–74.
[30] Johnson WP et al. Ferrographic tracking of bacterial transport in the field at the Narrow Channel Focus Area, Oyster, VA. Environ Sci Technol 2001;35:182–91.
[31] Drake LA et al. Potential invasion of microorganisms and pathogens via 'interior hull fouling': biofilms inside ballast water tanks. Biol Invasions 2005;7:969–82.
[32] Zborowski M et al. Immunomagnetic isolation of magnetoferritin-labeled cells in a modified ferrograph. Cytometry 1996;24:251–9.
[33] Fang B, Zborowski M, Moore LR. Detection of rare MCF-7 breast carcinoma cells from mixture of human peripheral leukocytes by magnetic deposition analysis. Cytometry 1999;36:294–302.
[34] Meyer DM, Tillinghast A, Hanumara NC, Franco A. Bio-ferrography to capture and separate polyethylene wear debris from hip simulator fluid and compared with conventional filter method. J Tribol 2006;128:436–41.
[35] Ishay JS et al. Gravity orientation in social wasp comb cells (Vespinae) and the possible role of embedded minerals. Naturwissenschaften 2008;95:333–42.
[36] Bowen ER, Westcott VC. Wear Particle Atlas (Revised). Lakehurst, NJ: Naval Air Engineering Center; 1976.
[37] Hughes S, Sweetnam R. The basis and practice of orthopaedics. London: Heinemann; 1980.
[38] Eliaz N. Electrocrystallization of calcium phosphates. Isr J Chem 2008;48:159–68.
[39] Oegema TR, Carpenter RJ, Hofmeister F, Thompson RC. The interaction of the zone of calcified cartilage and subchondral bone in osteoarthritis. Microsc Res Tech 1997;37:324–32.
[40] Barnes PRF, Mulvaney R, Wolff EW, Robinson K. A technique for the examination of polar ice using the scanning electron microscope. J Microsc 2002;205:118–24.
[41] Russ JC. Computer assisted microscopy. New York: Plenum Press; 1990.
[42] Jeffery AK et al. Three-dimensional collagen architecture in bovine articular cartilage. J Bone Joint Surg (Br) 1991;73-B:795–801.
[43] Yavorskyy A, Hernandez-Santana A, McCarthy G, McMahon G. Detection of calcium phosphate crystals in the joint fluid of patients with osteoarthritis – analytical approaches and challenges. Analyst 2008;133:302–18.
[44] Lagier R, Baud CA. Magnesium whitlockite, a calcium phosphate crystal of special interest in pathology. Pathol Res Pract 2003;199:329–35.
[45] Meshitsuka S et al. Trace element concentrations in synovial fluid of rheumatoid arthritis and osteoarthritis and its multivariate analysis. Yonago Acta Medica 1996;37:213–8.
[46] Milne AD, Evans NA, Stanish WD. Nonoperative management of knee osteoarthritis: Diagnosis, behavior modification, and pharmacologic options. Women's Health Primary Care 2000;3:841–6.